Electronic Supplementary Material (ESI) for Physical Chemistry Chemical Physics.
This journal is © the Owner Societies 2021

## Supplementary Information for:

# On the effect of metal loading on the reducibility and redox chemistry of ceria supported Pd catalysts

**Adam H. Clark,[a #] Huw R. Marchbank,[a##] David Thompsett,[b] Janet M. Fisher,[b] Alessandro Longo[c,d] Kevin A. Beyer,[e] Timothy I. Hyde,[b] Gopinathan Sankar[a]***

a. Department of Chemistry, University College London, 20 Gordon Street, London WC1H 0AJ, UK

b. Johnson Matthey Technology Centre, Blount's Court, Sonning Common, Reading RG4 9NH, UK.

c. I20, ESRF-The European Synchrotron, CS40220, 38043 Grenoble, Cedex 9, France.

d. CNR-ISMN, Consiglio Nazionale delle Ricerche, Istituto per lo Studio dei Materiali Nanostrutturati, Via Ugo La Malfa 153, 90146 Palermo, Italy.

e. X-ray Science Division, Advanced Photon Source, Argonne National Laboratory, USA

#. Current address: Paul Scherrer Institut, Villigen, CH-5232 Switzerland.

## Current Address : Johnson Matthey Technology Centre, Blount's Court, Sonning Common, Reading RG4 9NH, UK

## Table of contents.

In Figure **S1** we show the XRD data collected on the as received high surface area (HAS) ceria, 1% Pd and 5% Pd loaded samples demonstrating the samples are phase pure with no reflections relating to metallic or oxidic Pd or impurity phases. Analysis of both the ceria average crystallite size performed using the LVol-IB method and the ceria lattice parameter are reported in Table T1.

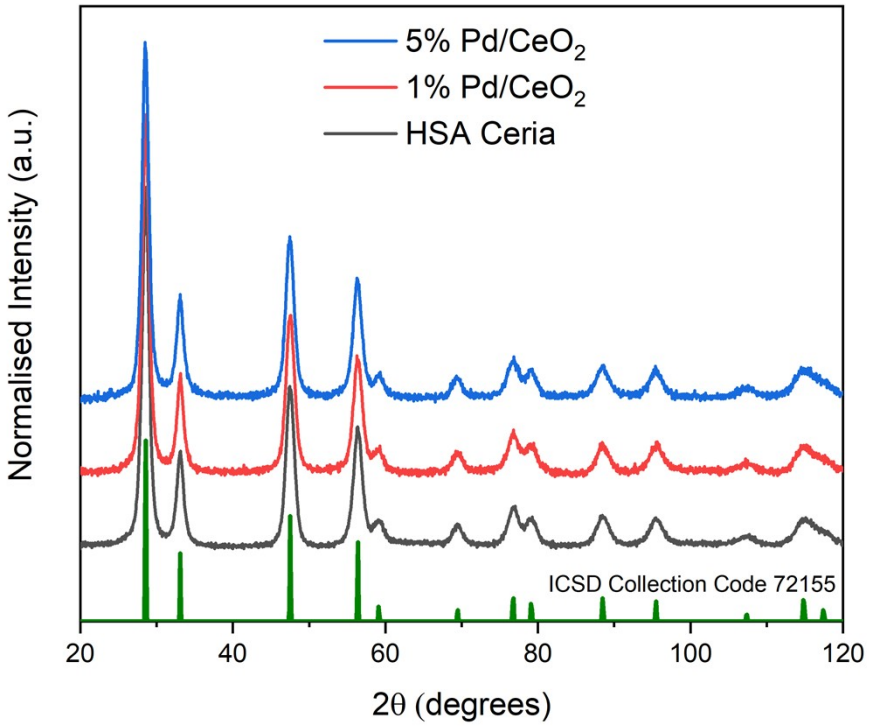


Figure S1. XRD data recorded on a Bruker AXS D8 diffractometer with a Cu Kα source on the as received samples along with a theoretical diffraction pattern of a fluorite ceria phase beneath.

Table T1. Rietveld refined cubic ceria XRD lattice parameters and average ceria crystallite size obtained from the LVol-IB method.

| **Sample** | **Lattice Parameter (Å)** | **Average Crystallite Size (nm)** |
|---|---|---|
| HSA Ceria | 5.4117(4) | 5.31(6) |
| 1%Pd/$CeO_2$ | 5.4127(5) | 5.29(8) |
| 5%Pd/$CeO_2$ | 5.4151(5) | 5.38(9) |

ICP analysis reporting the Pd content and impurity content of the high surface area ceria support are given in Tables **T2** and **T3** respectively.

Table T2. ICP analysis for Pd content of samples.

| **Sample** | **Pd (wt%)** |
|---|---|
| 1%Pd/$CeO_2$ | 1.02 |
| 5%Pd/$CeO_2$ | 4.73 |

Table T3. ICP analysis listing the impurity content of the high surface area ceria support.

| Impurity | ppm |
|---|---|
| Al | ≤20 |
| Ba | 1 |
| B | ≤10 |
| Ca | ≤10 |
| Cu | ≤1 |
| Fe | 15 |
| Ga | ≤5 |
| Ge | ≤5 |
| K | ≤10 |
| La | ≤30 |
| Mn | ≤1 |
| Na | ≤10 |
| Nd | ≤20 |
| Ni | ≤1 |
| P | 180 |
| Pr | ≤30 |
| S | ≤50 |
| Si | 55 |
| Ti | 1 |
| V | 10 |
| W | ≤10 |
| Zr | ≤10 |

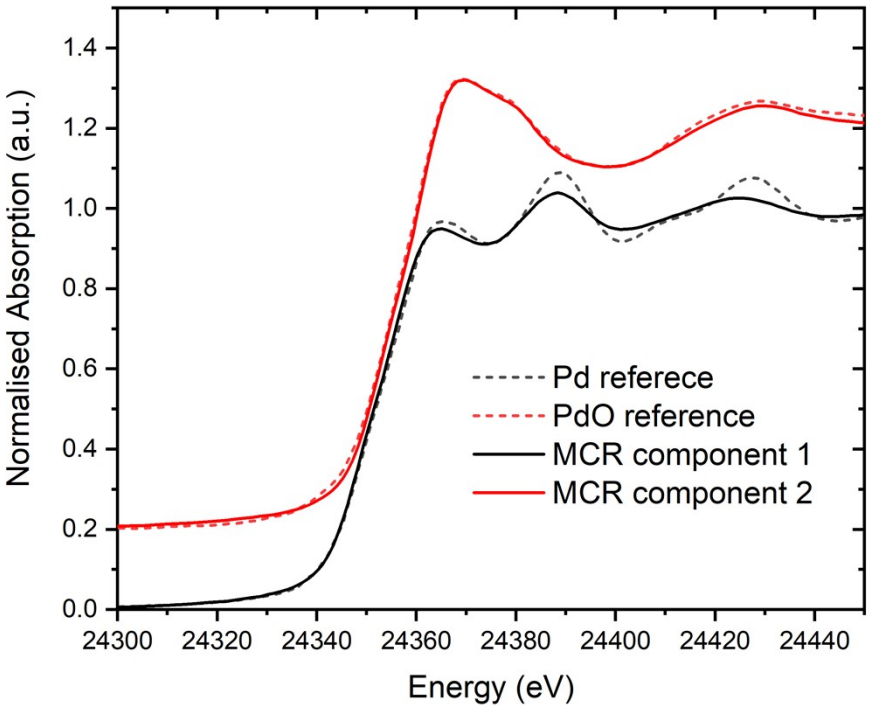


Figure S2. Comparison of the components extracted with MCR analysis for the in situ Pd K-edge XANES analysis with standard reference materials.

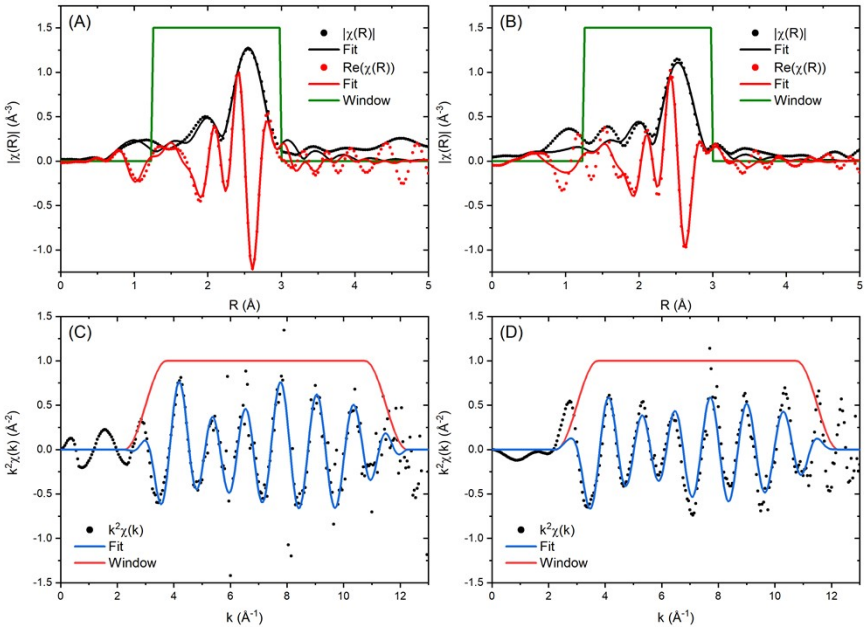


Figure S3. Fitting of the EXAFS after reduction in 5% $H_2/N_2$ at 450 °C and cooled to room temperature giving the R space and K space fitting in (A) and (C) for the 1wt% $Pd/CeO_2$ sample and in Figures (B) and (D) for the 5 wt% $Pd/CeO_2$ sample

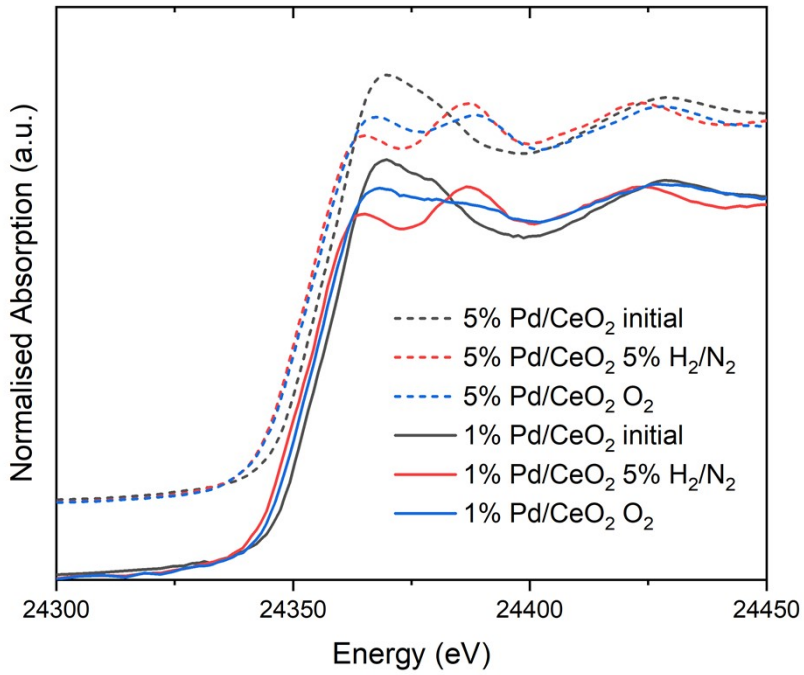


Figure S4. Example Pd K-edge data showing the MCR analysis of the 1 wt% $Pd/CeO_2$ sample for the initial, after reduction in 5% $H_2/N_2$ at 450 °C, cooled to 30 °C in 5% $H_2/N_2$, after passivation with synthetic air and after the second reduction in 5% $H_2/N_2$ at 100 °C spectra in black, red, blue, green and purple respectively.

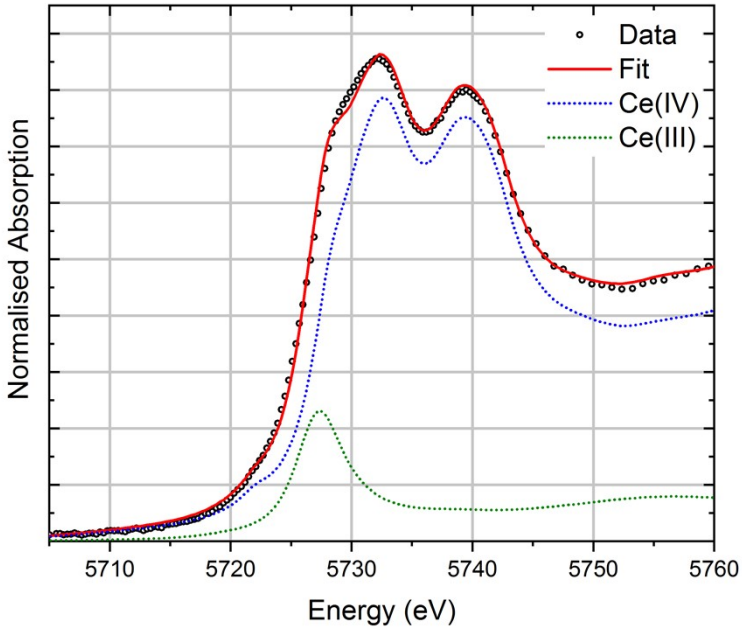


Figure S5. Example LCF Analysis performed on the Ce $L_3$-edge. Green and blue dashed line gives the concentration weighted component fractions for the Ce(III) standard material (cerium nitrate hexahydrate) and the Ce(IV) standard material (calcined bare ceria support) respectively.

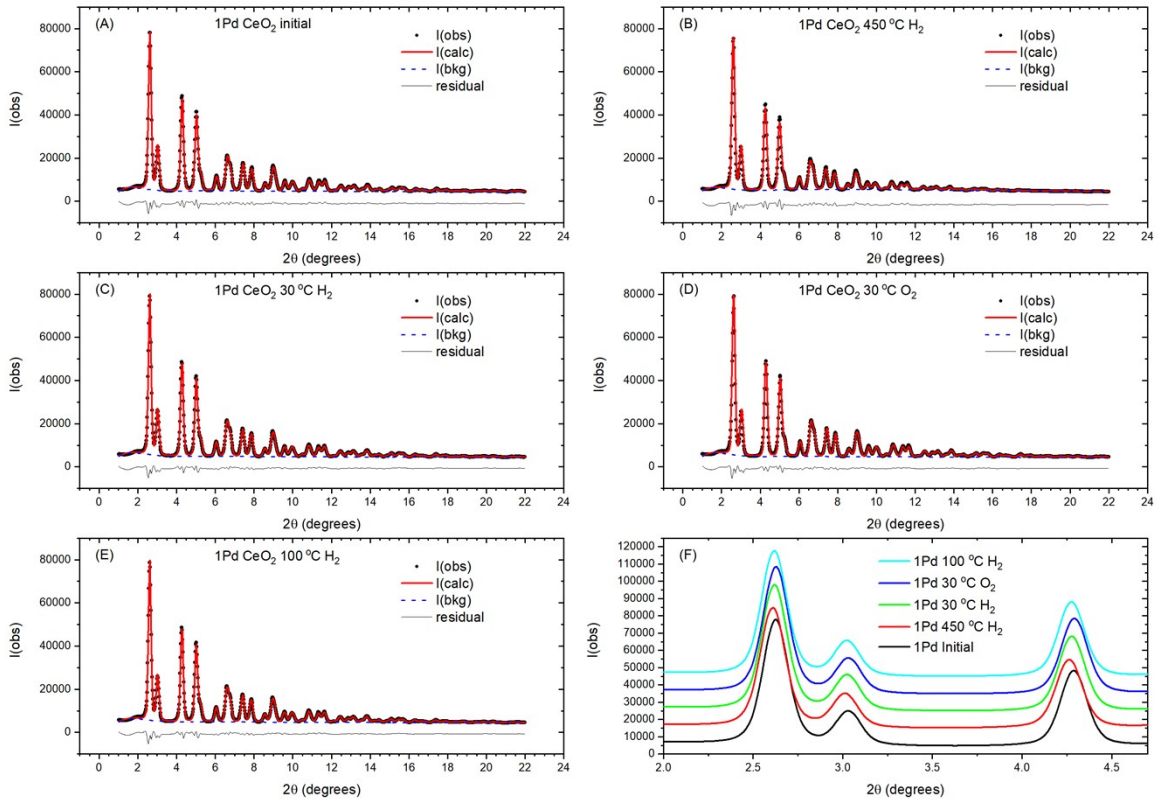


Figure S6. Examples of Rietvend analysis fitting quality achieved for the 1 wt% Pd/$CeO_2$ sample different points in the experiment cycle, the most prevalent phase is fluorite $CeO_2$ in all cases. (A) initial as received sample (B) after heating to 450 °C in 5%$H_2$/$N_2$ (C) after cooling to 30 °C in 5% $H_2$/$N_2$ (D) after passivation in $O_2$ (E) after heating for a second time in 5%$H_2$/$N_2$ to 100 °C (F) zoomed in view of a stacked plot showing the absence of an observable Pd(111) reflection.

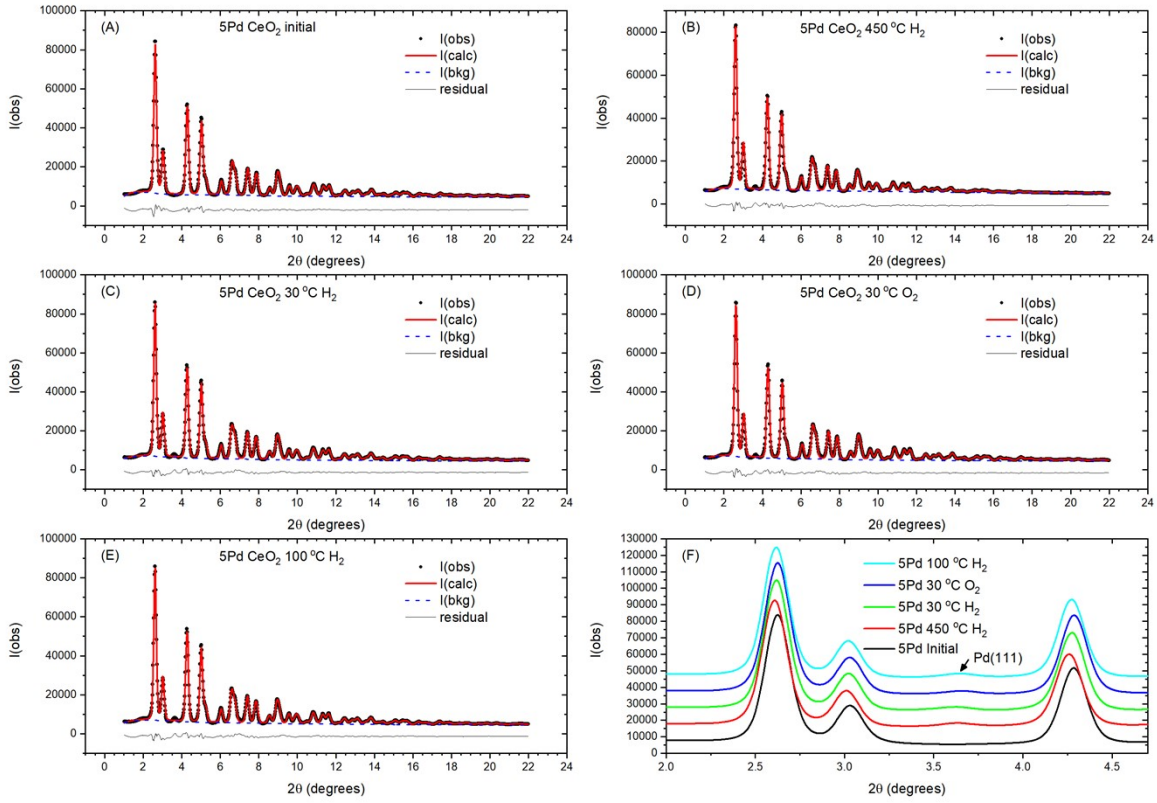


Figure S7. Examples of Rietvend analysis fitting quality achieved for the 5 wt% $Pd/CeO_2$ sample different points in the experiment cycle, the most prevalent phase is fluorite $CeO_2$ in all cases. (A) initial as received sample (B) after heating to 450 °C in 5%$H_2/N_2$ (C) after cooling to 30 °C in 5% $H_2/N_2$ (D) after passivation in $O_2$ (E) after heating for a second time in 5%$H_2/N_2$ to 100 °C (F) zoomed in view of a stacked plot showing the formation of a weak Pd(111) reflection.

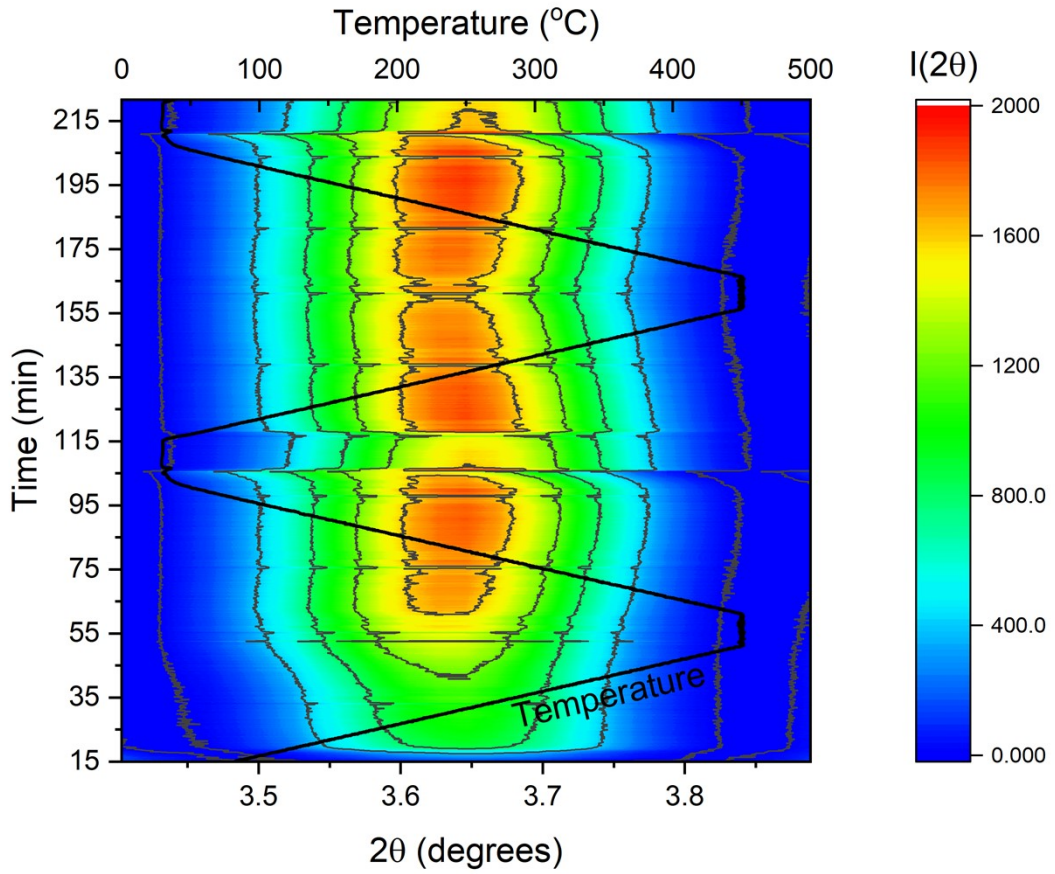


Figure S8. Surface colour contour plot showing the variation in intensity after background subtraction of the Pd(111) reflection for the 5 wt% Pd/$CeO_2$ sample during 2 full experimental cycles

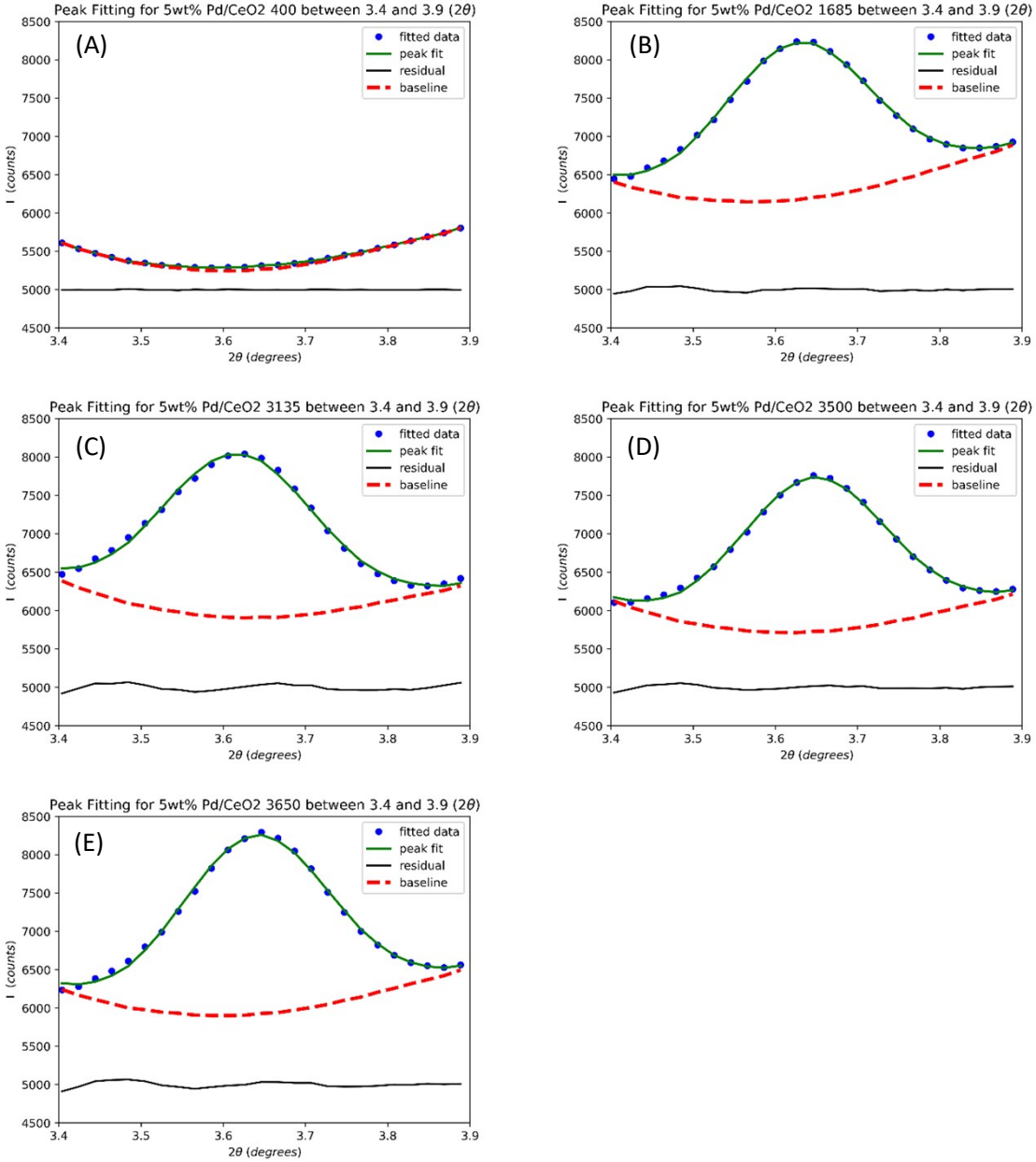


Figure S9. Example peak fitting applied to 5 wt% $Pd/CeO_2$ sample for the Pd(111) reflection showing the data as blue points, the refined background as red dashed line and the fit to the data as the green solid lines. (A) sample at the onset of metallic Pd formation at approximately 80 $^oC$ (B) after heating to 450 $^oC$ in 5%$H_2/N_2$ (C) after cooling to 30 $^oC$ in 5% $H_2/N_2$ (D) after passivation in $O_2$ (E) after heating for a second time in 5%$H_2/N_2$ to 100 $^oC$

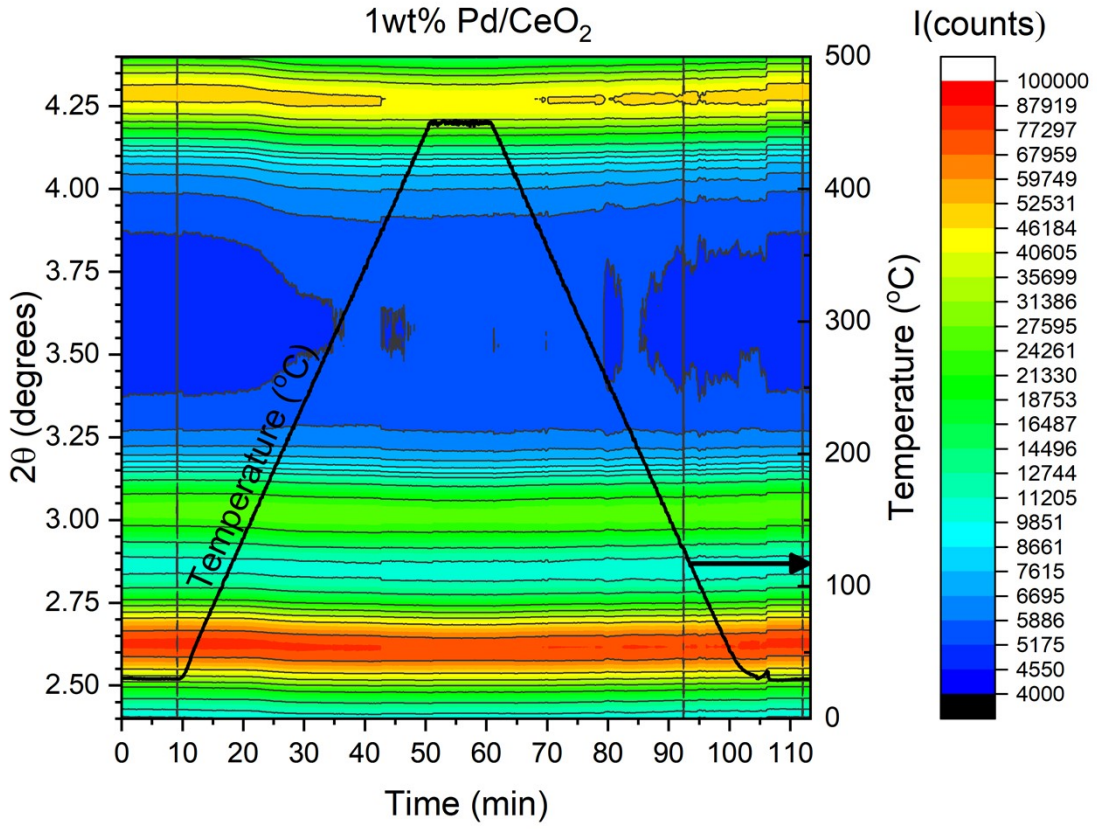


Figure S10. Surface colour contour plot showing the variation in intensity in the region of the Pd(111) reflection for the 1 wt% $Pd/CeO_2$ sample showing no observable formation of crystalline metallic Pd